Synthesis, Docking, and Bioavailability of 2′-Oxo-3-phenylspiro[cyclopropane-1,3′-indoline]-2,2-dicarbonitriles as Antibacterial Agents *In Silico*

Vijay Kumar Reddy Avula,[a,b] Venkata Ramaiah Chintha,[c] Swetha Vallela,[b] Jaya Shree Anireddy,[b] Naga Raju Chamarthi,[a*] and Rajendra Wudayagiri[c]

[a]Department of Chemistry, Sri Venkateswara University, Tirupati, Andhra Pradesh 517502, India
[b]Centre for Chemical Sciences and Technology, Institute of Science and Technology, Jawaharlal Nehru Technological University, Hyderabad, Kukatpally, Telangana 500085, India
[c]Department of Zoology, Sri Venkateswara University, Tirupati, Andhra Pradesh 517502, India
*E-mail: rajuchamarthi10@gmail.com

Received May 27, 2018
DOI 10.1002/jhet.3396
Published online 00 Month 2018 in Wiley Online Library (wileyonlinelibrary.com).

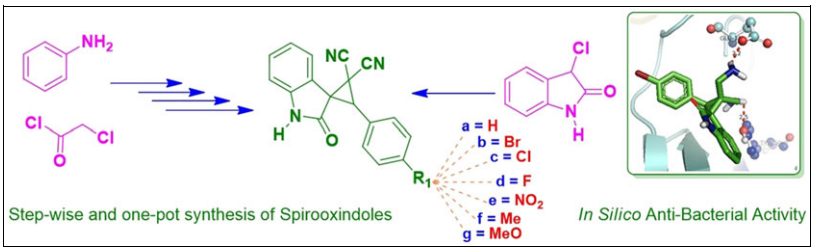

An efficient method has been developed for the synthesis of *N*-alkylated 2′-oxo-3-phenylspiro[cyclopropane-1,3′-indoline]-2,2-dicarbonitrile from 3-chloroindolin-2-one and 2-benzylidenemalononitrile by using triethylamine as a base at room temperature and obtained the products in moderate to good yields. In extension, the scope of the reaction has been investigated by stepwise and one-pot methods. Furthermore, *in silico* antibacterial activity was carried out in order to understand possible binding modes of novel derivatives with the active site of DNA gyrase A enzyme, and the results were well complemented. Additionally, absorption, distribution, metabolism, and excretion properties of compounds have shown drug likeness with good oral absorption and moderate blood–brain barrier permeability.

INTRODUCTION

The spirooxindole framework has remained a synthetically challenging and privileged architectural motif that is prevalent in many pharmaceuticals and bioactive natural products [1]. This class of frameworks has attracted more interest from chemists because of their biological importance and the challenge embedded in their synthesis [2]. The unique structures and the highly pronounced pharmacological activity displayed by the spirooxindoles have made them attractive synthetic targets [3]. As part of a medicinal chemistry project, we have been focusing on the synthesis of novel 3′-spirocyclo-oxindoles, and we recently reported the preparation of 3′-spiropentacyclo-oxindole derivatives using phosphine-catalyzed [3 + 2]-cycloaddition reactions [4]. Interestingly, when diphenyldiazomethane was employed, the desired 3,3-diphenyl-3′-spirocyclopropyloxindole-2-carboxylic ester [5] was obtained.

As synthetic tools, nitrile-substituted cyclopropanes are versatile templates for the rapid formation of biologically active and synthetically useful functionalized cyclopropane derivatives [6]. The synthesis of spirocycloindolones has shown great interest because they display a variety of biological activities and many of them used as starting materials for alkaloid synthesis [7]. Spirooxindoles are one of the most important classes of naturally occurring substances, characterized by highly pronounced biological properties. These molecules are also the core structure of many synthetic pharmaceuticals [8]. While the synthesis of spirocyclic oxindoles has continued to gain attention, the development of enantioselective methods to access spirooxindoles remains an ongoing synthetic challenge. This review features recent strategies for the enantioselective synthesis of spirocyclic oxindoles, focusing on reports from 2010 and 2011 [9]. An extensive investigation on this aspect of isatins' chemistry during the past decade has led to successful design and synthesis of diverse types of heterocyclic and carbocyclic compounds with a spiro-fused 2-oxindole ring containing many stereocenters on one hand and discovery of many interesting facts of organic synthesis design on the other hand that need to be comprehensively reviewed [10].

On the other hand, the general synthetic routes to 1-arylcyclopropane-1,2-dicarboxylate derivatives involve the reaction of α-bromophenylacetates with acrylic esters under strong basic conditions [11]. Organocatalytic

approaches to spiro-annulation of oxindoles offer a high degree of stereoenantio control and have become extremely popular for the construction of five-membered and six-membered spiro-rings [12–18]. Artur Noole *et al.* [19] reported highly enantio and diastereoselective generation of two quaternary centers in spirocyclopropanation of oxindole derivatives. Artur Nool *et al.* [20] described asymmetric organometalic synthesis of spiro cyclopropaneoxindoles using thiourea-based catalyst emerged as the most suitable, providing the spiro-cyclopropaneoxindole in excellent enantioselectivity and diastereoselectivity and in almost quantitative yield. Erin *et al.* [21] described stereochemical implications in the synthesis of spirocyclopropyl oxindoles from β-aryl/alkyl-substituted alkylidene. Rong Zhou *et al.* [22] reported $P(NMe_2)_3$-mediated model reaction between and afforded the expected cyclopropanation product. Wen-Jie *et al.* [23] reported a new method for the synthesis of functionalized spiro cyclopropane indoline. John *et al.* [24] reported the synthesis of gem-dimethyl cyclopropane using isopropyl triphenylphoshorane as a catalyst and MeI as an alkylating agent in tetrahydrofuran solvent. The synthesized molecules are subjected to the molecular docking active binding pocket of the DNA gyrase A enzyme. Moreover, we have also used an *in silico* method to predict absorption, distribution, metabolism, and excretion (ADME) properties, in order to suggest the suitability of the new compounds for further drug development with respect to antibacterial activity.

RESULTS AND DISCUSSION

Chemistry. Based on the earlier literature, we developed a new method for the synthesis of spiro cyclopropane indoline derivatives using different solvents and bases. The simple and commercially available starting materials aniline and chloroacetyl chloride were reacted by using K_2CO_3 base in dichloromethane (DCM) solvent in the presence of aluminium trichloride to give corresponding **3** [25] was shown in Scheme 1. On further treatment of 3 with CMOBSC (chloromethoxy benzenesulfonic acid) in acetonitrile solvent to obtain chloro oxindole **4** [26]. Further, it was treated with substituted 2-benzylidenemalononitriles in the presence of triethylamine in toluene solvent at room temperature for overnight to afford the corresponding title compounds (**8a–g**) in very poor yield. In order to improve the yields and optimize the reaction conditions, different solvents and bases were tried. Among those conditions, triethylamine as a base and DCM as a solvent at room temperature for overnight gave an excellent yield; hence,

Scheme 1. Stepwise and one-pot synthesis of 2′-oxo-3-phenylspiro[cyclopropane-1,3′-indoline]-2,2-dicarbonitriles (**8a–g**). DCM, dichloromethane; RT, room temperature. [Color figure can be viewed at wileyonlinelibrary.com]

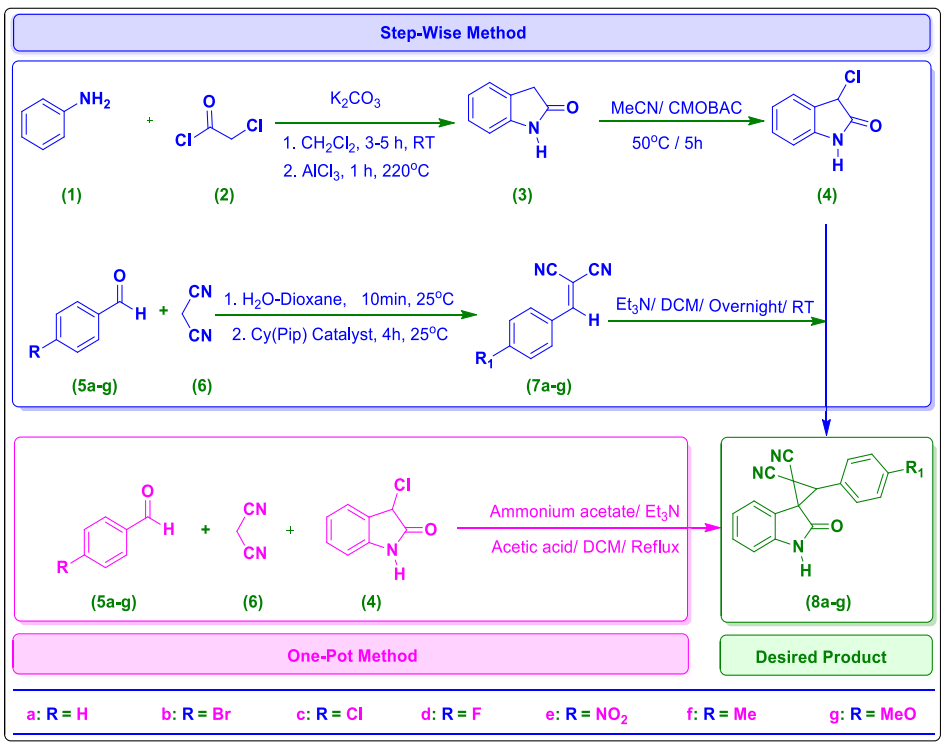

this methodology has been adopted for the synthesis of other derivatives. The structures of title compounds were confirmed by NMR and mass spectral data.

The title compounds could also be prepared in one-pot method as shown in Scheme 1. The synthesis of 2′-oxo-3-phenylspiro [cyclopropane-1,3′-indoline]-2,2-dicarbonitrile *via* one-pot and three-component method using starting materials substituted benzaldehydes, malononitrile, and 3-chloro oxindole in the presence of ammonium acetate, triethylamine as a base in DCM solvent, and acetic acid under reflux conditions to obtain moderate to good yields. Stepwise synthesis gave good yields compared with one-pot, three-component method, and these results are given in Tables 1 and 2. The detailed comparative yields were tabulated in Table 3, respectively, for stepwise and one-pot methods.

Molecular docking. The docking protocol was validated using redocking experiments by removing the native ligand from DNA gyrase A and redocked into the same binding pocket using Auto Dock 4.2 in PyRx with default parameters. It showed a root-mean-square deviation value of 0.689 Å, to obtain from all atoms and heteroatom coordinates between experimental and redocked confirmations. Moreover, the docked native ligand is bound tightly to DNA gyrase A involving almost the same residues as in the co-crystallized structure. This indicates that these parameters are adequate in reproducing the experimental structure and can be extended to do docking studies on our synthesized compounds. The molecular docking results revealed that all the compounds **8a–g** tend to bind within the binding pocket of DNA gyrase A and show good binding energies ranging from −7.2 to −6.4 kcal/mol. The docking results are summarized in Table 4.

Compound **8a** showed the highest binding energy of −7.2 kcal/mol and the lowest inhibition constant of 0.82 followed by compounds **8b**, **8d**, and **8g**, which showed binding energies of −7.0, −6.8, and −6.8 kcal/mol and inhibition constants of 1.13 and 1.53, respectively. The low inhibition constant and more negative value of binding energy indicate good binding affinity of the ligand towards the target enzyme. Thus, the results correlate well with the observed *in silico* antibacterial activity. The three-dimensional visualization of the interactions of the most active compounds **8a**, **8b**, **8d**, **8f**, and **8g** within the binding pocket of DNA gyrase A is shown in Figure 1.

The binding models indicate that the compounds are held in the active site by a combination of various hydrogen bonding and hydrophobic interactions. Single hydrogen bond was present in the derivative of **8a**, which has the highest binding energy among the series. It showed hydrogen bonding interaction with amino acid residue Asp 104 at the bond distances of 2.3 Å, respectively. This is evidence for the requirement of hydrophilic groups to bind strongly to the protein active site. Whereas the remaining active compounds such as **8d**, **8b**, **8g**, and **8f** showed the interactions with amino acids Val 103, Glu 139, Tyr 50, and Arg 126 at a bond distance 2.7, 2.2, 2.5, 2.1, 2.5, 2.4, and 2.7, respectively.

Bioavailability of compounds 8a–g. Nowadays, many potential drugs fail to reach the clinic because of ADMET liabilities. Absorption, distribution, metabolism, excretion, and toxicity (ADMET) processes play a pivotal

Table 1

Optimization of reaction conditions at RT with TEA base (conc: 0.2 mole equiv).

S. no.	Solvent	Time (h)	Yield (%)
1	Toluene	12	20
2	Acetonitrile	12	50
3	DMF	12	35
4	DMSO	12	40
5	Ethanol	12	25
6	Methanol	12	20
7	THF	12	35
8	1,4-Dioxane	12	25
9	$CHCl_3$	12	75
10	DCM	12	90

DCM, dichloromethane; DMF, dimethylformamide; DMSO, dimethyl sulfoxide; RT, room temperature; TEA, triethylamine; THF, tetrahydrofuran.

Table 2

Optimization of reaction conditions with different bases at RT in DCM solvent.

S. no.	Base (equiv 0.2)	Time (h)	Yield (%)
1	Pyridine	12	10
2	Morpholine	12	15
3	*N*,*N*-Diethylamine	12	20
4	Piperidine	12	25
5	Triphenylphosphine	12	Nil
6	Ammonium acetate	12	Nil
7	Sulfamic acid	12	Nil
8	L-Proline	12	20
9	Ammonia	12	Nil
10	TEA	12	90

DCM, dichloromethane; RT, room temperature; TEA, triethylamine.

Table 3

Comparative parameters of stepwise and one-pot method.

Compound	**8a**	**8b**	**8c**	**8d**	**8e**	**8f**	**8g**
% of yield in stepwise method	90	89	85	80	70	80	80
% of yield in one-pot method	80	75	70	65	60	65	65

Table 4

Bonding characterization of synthesized compounds (**8a–g**) and Nfx (one reference drug) against *Escherichia coli* DNA gyrase A protein.

Compound	Rank	BE (kcal/mol)	Binding interaction	Bond length (Å)	Bond angle (°)	Bond type
8a	1	−7.2	Asp 104 CG···HN	2.3	108.4	H– don
8b	3	−6.8	Glu 139 CD···HN	2.2	126.2	H– don
			Tyr 50 CZ···HN	2.5	120.5	H– don
8c	7	−6.4	Met 101 CG···HN	2.1	112.8	H– don
8d	2	−7.0	Val 103 CA···HN	2.7	122.8	H– don
8e	6	−6.5	Glu 141 CZ···HN	2.3	128.8	H– don
8f	5	−6.7	Arg 126 CB···HN	2.7	118.6	H– don
8g	4	−6.8	Glu 139 CD···HN	2.5	126.2	H– don
			Tyr 50 CZ···HN	2.4	120.5	H– don
Nfx	R	−6.6	Phe 213 CB···HN	2.6	104.7	H– don
			Asp 104 CG···HO	1.8	116.6	H– don
			Trp 59 CA···HO	2.1	120.5	H– don

BE, binding energy.

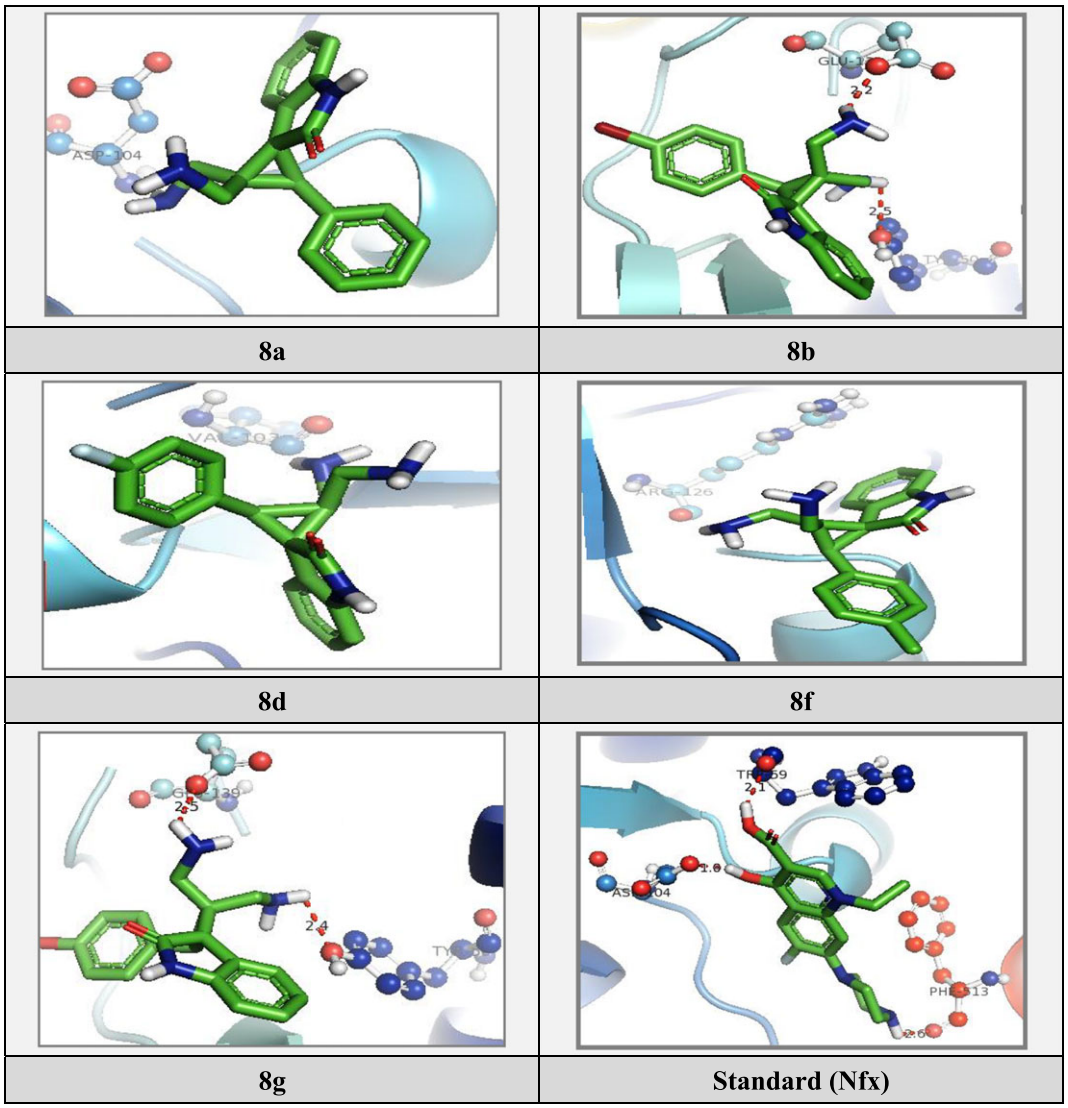

Figure 1. Diagram representing the three-dimensional modeled binding modes of compounds **8a**, **8b**, **8d**, **8f**, **8g**, and Nfx (standard) within the binding domain of DNA gyrase A. [Color figure can be viewed at wileyonlinelibrary.com]

Table 5

Physicochemical properties of compounds **8a–g**.

Compound	MW	MV	NRB	NHBD	NHBA	LROWPC	TPSA	LV	PA
Rule	≤500	—	—	≤5	≤10	≤5	—	≤1	—
8a	390.2	336.6	5	0	8	3.42	80.46	0	90.5
8b	378.6	354.0	6	0	7	3.26	82.18	0	90.5
8c	349.8	373.4	5	0	8	3.28	88.42	0	97.3
8d	422.6	372.4	5	0	77	3.35	84.66	0	90.5
8e	450.4	313.9	5	0	8	3.45	86.12	0	74.7
8f	347.8	341.0	5	0	7	3.96	90.36	0	90.5
8g	340.6	303.3	5	0	7	4.10	82.14	0	90.5

MW, molecular weight; MV, molecular volume; NRB, number of rotatable bonds; NHBD, number of hydrogen bond donors (–OH and –NH); NHBA, number of hydrogen bond acceptors; LROWPC, logarithmic ratio of the octanol–water partitioning coefficient; TPSA, topological polar surface area; LV, Lipinski's violation; PA, percentage of absorption %ABS = 109 − (0.3459 TPSA).

role in defining the therapeutic efficacy of a drug. Drug likeness appears as a promising paradigm of a compound that optimizes their ADME in the human body [27]. With the aim of estimating the drug likeness of the compounds, we have determined the compliance of the synthesized molecules to the Lipinski's "rule of five." According to this rule, poor absorption or permeation is more likely when there are more than five hydrogen bond donors and 10 hydrogen bond acceptors, the molecular weight is greater than 500, and the calculated log *p* (logarithmic ratio of the octanol–water partitioning coefficient) is greater than 5. Molecules violating more than one of these parameters may have problems with bioavailability and a high probability of failure to display drug likeness [28]. Further, the topological polar surface area (TPSA), which is another key property in estimating drug bioavailability, was also calculated. Generally, compounds with a TPSA ≥ 140 $Å^2$ are thought to have low bioavailability [29]. As shown in Table 5, all the synthesized compounds comply with these rules. Moreover, the compounds exhibited a greater percentage of absorption (%ABS) ranging from 74.70 to 90.5%. Hence, theoretically, all of these compounds have good passive oral absorption and drug likeness.

Table 6

Prediction of pharmacokinetic properties of compounds **8a–g**.

Compound	Caco-2 permeability	HIA (%)	PPB (%)	BBB
8a	20.36	98.14	94.16	0.112
8b	22.18	98.6	92.28	0.452
8c	21.12	98.46	93.36	0.444
8d	20.86	99.12	93.38	0.136
8e	26.24	99.36	94.46	0.432
8f	23.86	98.89	98.88	0.224
8g	22.14	98.84	100.00	0.428

Caco-2, colon adenocarcinoma; HIA, human intestinal absorption; PPB, plasma protein binding; BBB, blood–brain barrier ($C_{brain}C_{blood}$).

In addition to this, some ADME predictions such as blood–brain barrier (BBB) penetration, % of human intestinal absorption (HIA), Caco-2 permeability, and % of PPB were predicted for all compounds. Analysis of ADME predictions (Table 6) reveals that all the compounds showed high % of HIA in the range of 98.14–99.36% and is well absorbed. The Caco-2 cell permeability is moderate, ranging from 20.36 to 26.24 nm/

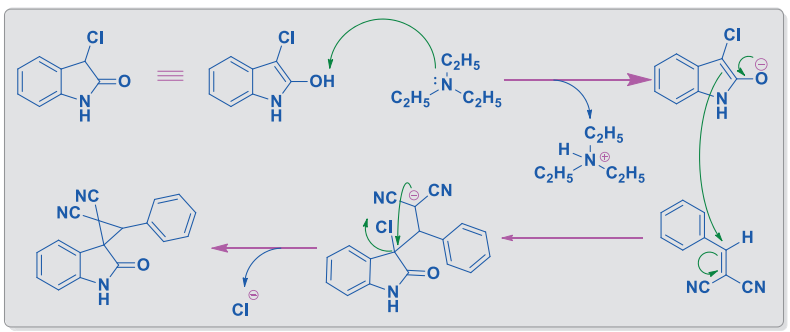

Figure 2. Plausible reaction mechanism for the formation of spirooxindoles. [Color figure can be viewed at wileyonlinelibrary.com]

s. Furthermore, all of them are strongly bound to plasma proteins with %PPB penetration more than 92.28%, and they were also found to have moderate penetration (0.112–0.452) to the central nervous system through the BBB. Hence, it can be stated that, theoretically, all the compounds exhibited good absorption and bioavailability with reasonable permeability through the BBB.

CONCLUSION

We have developed a new synthetic methodology for spiro cyclopropane indoline derivatives (**8a–g**) by using a new and stable and economically affordable chlorinating reagent (*N*-chloro-*N*-methozxybenzenesulfonamide) and compared the yields in both stepwise and one-pot methods by using optimized conditions. As an addition, molecular docking studies of the synthesized compounds **8a–g** against DNA gyrase A enzyme revealed that compounds such as **8a**, **8d**, **8b**, **8g**, and **8f** showed higher binding affinities and many more interactions when compared with other compounds. In addition, *in silico* ADME prediction showed that all the compounds fulfilled Lipinski's rule of five with moderate potential to penetrate the BBB. These results suggested that compounds **8a**, **8d**, **8b**, **8g**, and **8f** can be considered as promising candidates for further development of potential antibacterial drugs.

EXPERIMENTAL

All the starting materials and solvents were purchased in reagent grade and used as such, and products were purified by column chromatography (silica gel 200–300). Melting points were determined in open capillary tubes using Guna digital melting point apparatus (Hyderabad, India). Thin-layer chromatography (TLC) analyses were run on silica gel-G, and visualization was performed using UV lamp (Hyderabad, India) or iodine. ^{1}H-NMR and ^{13}C-NMR spectra were recorded on Bruker 400-MHz instrument (Ettlingen, Germany) in $CDCl_3$ or DMSO-d_6 using tetramethylsilane (TMS) as an internal standard at 400 and 100 MHz, respectively. Chemical shifts were recorded on δ scale in parts per million (ppm). Mass spectra were recorded on Agilent LCMS instrument (Ettlingen, Germany).

General procedure for the synthesis of title compounds (8a–g) in stepwise method. A solution of chloro oxindole (**4**, 10 mmol), substituted benzonitriles (**7a–g**, 10 mmol), and triethylamine catalytic amount (0.2 mmol) in DCM solvent was taken in a 100-mL round bottom flask reacted at RT and monitored the progress of the reaction by TLC. After completion of reaction, the reaction mass was concentrated under vacuum and purified by column chromatography (1:9 ethyl acetate and hexane).

General procedure for the synthesis of title compounds (8a–g) in one-pot method. A solution of chloro oxindole (**4**, 10 mmol), substituted benzaldehyde (**5a–g** 10 mmol), malononitrile (**6**, 10 mmol), and triethylamine catalytic amount (0.2 mmol) in the presence of acetic acid (10 mL) in DCM solvent was taken in a 100-mL round bottom flask and refluxed for 12 h. The consumption of starting material was monitored by TLC. After completion of the reaction, obtained mass was concentrated under vacuum and purified by column chromatography (1:9 ethyl acetate and hexane). The plausible reaction mechanism was provided in Figure 2.

Spectral data of title compounds (8a–g). ***2-(2′-Oxo-2-phenylspiro[cyclopropane-1,3′-indolin]-3-yl)malononitrile (8a).*** White solid, yield = (92%); mp 147–149°C, IR (KBr) (ν_{max}/cm^{-1}): 3033, 2952, 2242, 1725, 1619, 1491, 1445, 1351, 1272, 1181, 1124, 1016, 821, 695 cm^{-1}; ^{1}H-NMR (400 MHz, $CDCl_3$/TMS): δ 3.9 (s, 1H, CH), 6.89–7.04 (m, 1H, Ar–H), 7.18–7.25 (m, 2H, Ar–H), 7.32–7.44 (m, 6H, Ar–H), 8.90 (s, 1H, –NH); ^{13}C-NMR (400 MHz, $CDCl_3$): 20.04, 39.84, 42.83, 110.1, 111.4, 116.2, 116.5, 121.2, 121.8, 122.7, 123.2, 125.5, 130.5, 131.2, 141.4, 142.0, 168.4: MS (negative mode): *m/z* = 284 [M + H]$^+$. Anal. Calcd (%) for $C_{18}H_{11}N_3O$: C, 75.78; H, 3.89; N, 14.73. Found: C, 75.68; H, 3.82; N, 14.65.

2-(2-(4-Bromophenyl)-2′-oxospiro[cyclopropane-1,3′-indolin]-3-yl)malononitrile (8b). Pale yellow solid, yield = (90%); mp 202–204°C, IR (KBr) (ν_{max}/cm^{-1}): 3029, 2949, 2241, 1719, 1620, 1489, 1446, 1352, 1271, 1179, 1124, 1019, 826, 691 cm^{-1}; ^{1}H-NMR (400 MHz, $CDCl_3$/TMS): δ 2.09 (s, 1H, CH), 6.34–6.35 (d, 1H, Ar–H), 6.95–6.98 (t, 2H, Ar–H), 7.09–7.12 (t, 2H, Ar–H), 7.37–7.40 (t, 2H, Ar–H), 7.56–7.57 (d, 2H, Ar–H), 8.50 (s, 1H, –NH); ^{13}C-NMR (400 MHz, $CDCl_3$): 32.91, 39.91, 65.90, 110.1, 110.0, 116.1, 116.5, 118.1, 121.9, 122.8, 125.5, 130.6, 131.3, 131.8, 132.0, 170.4: MS (positive mode): *m/z* = 366 [M + H]$^{+2}$. Anal. Calcd (%) for $C_{18}H_{10}BrN_3O$: C, 59.36; H, 2.77; N, 11.54. Found: C, 59.42; H, 2.72; N, 11.45.

2-(2-(4-Chlorophenyl)-2′-oxospiro[cyclopropane-1,3′-indolin]-3-yl)malononitrile (8c). White solid, yield = (90%); mp 181–182°C, IR (KBr) (ν_{max}/cm^{-1}): 3021, 2915, 2235, 1718, 1622, 1451, 1461, 1352, 1252, 1150, 1109, 1028, 820, 693 cm^{-1}; ^{1}H-NMR (400 MHz, $CDCl_3$/TMS): δ 3.97 (s, 1H, CH), 7.02–7.04 (m, 1H, Ar–H), 7.15–7.19 (m, 2H, Ar–H), 7.28–7.30 (m, 2H, Ar–H), 7.52–7.59 (m, 4H, Ar–H), 9.19 (s, 1H, –NH); ^{13}C-NMR (400 MHz, $CDCl_3$): 20.52, 40.21, 41.62, 111.4, 111.9, 115.5, 117.1, 120.9, 121.1, 122.5, 123.4, 123.9, 131.4, 133.1, 143.5, 144.0, 170.9: MS (positive mode): *m/z* = 321 [M + H]$^{+2}$. Anal. Calcd (%) for

$C_{18}H_{10}ClN_3O$: C, 67.61; H, 3.15; N, 13.14. Found: C, 67.56; H, 3.13; N, 13.21.

2-(2-(4-Fluorophenyl)-2′-oxospiro[cyclopropane-1,3′-indolin]-3-yl)malononitrile (8d). White solid, yield = (90%); mp 149–150°C, IR (KBr) (ν_{max}/cm^{-1}): 3012, 2931, 2236, 1720, 1625, 1461, 1451, 1332, 1222, 1170, 1106, 1029, 821, 691 cm^{-1}; ^{1}H-NMR (400 MHz, $CDCl_3$/TMS): δ 3.99 (s, 1H, CH), 6.92–6.98 (m, 1H, Ar–H), 7.12–7.42 (m, 8H, Ar–H), 9.21 (s, 1H, –NH); ^{13}C-NMR (400 MHz, $CDCl_3$): 19.92, 39.21, 40.62, 111.3, 111.2, 114.5, 115.1, 119.9, 120.1, 122.5, 123.5, 124.3, 130.4, 132.1, 142.5, 142.0, 168.9: MS (positive mode): m/z = 304 $[M + H]^+$. Anal. Calcd (%) for $C_{18}H_{10}FN_3O$: C, 71.28; H, 3.32; N, 13.85 Found: C, 71.18; H, 3.29; N, 13.92.

2-(2-(4-Nitrophenyl)-2′-oxospiro[cyclopropane-1,3′-indolin]-3-yl)malononitrile (8e). White solid, yield = (90%); mp 183–185°C, IR (KBr) (ν_{max}/cm^{-1}): 3025, 2948, 2231, 1718, 1621, 1469, 1441, 1342, 1262, 1180, 1109, 1023, 825, 681 cm^{-1}; ^{1}H-NMR (400 MHz, $CDCl_3$/TMS): δ 3.89 (s, 1H, CH), 7.02–7.09 (m, 1H, Ar–H), 7.15–7.19 (m, 3H, Ar–H), 7.91–7.97 (m, 2H, Ar–H), 8.31–8.35 (m, 2H, Ar–H), 9.12 (s, 1H, –NH); ^{13}C-NMR (400 MHz, $CDCl_3$): 20.3, 39.3, 41.9, 112.1, 112.9, 115.5, 116.2, 120.2, 120.8, 123.7, 124.2, 125.5, 131.5, 132.2, 143.4, 144.0, 169.4: MS (positive mode): m/z = 331 $[M + H]^+$. Anal. Calcd (%) for $C_{18}H_{10}N_4O_3$: C, 65.45; H, 3.05; N, 16.96 Found: C, 65.37; H, 3.12; N, 16.85.

2-(2′-Oxo-2-(p-tolyl)spiro[cyclopropane-1,3′-indolin]-3-yl) malononitrile (8f). White solid, yield = (90%); mp 164–165°C, IR (KBr) (ν_{max}/cm^{-1}): 3230, 3023, 2952, 2335, 1721, 1722, 1651, 1462, 1321, 1272, 1170, 1107, 1027, 827, 683 cm^{-1}; ^{1}H-NMR (400 MHz, $CDCl_3$/TMS): δ 3.97 (s, 1H, CH), 3.57 (s, 3H, CH_3), 6.95–7.00 (m, 1H, Ar–H), 7.17–7.20 (m, 2H, Ar–H), 7.39–7.44 (m, 6H, Ar–H), 9.5 (s, 1H, –NH); ^{13}C-NMR (400 MHz, $CDCl_3$): 17.3, 20.2, 40.2, 41.7, 111.6, 116.9, 116.5, 117.6, 120.3, 121.5, 122.6, 123.5, 123.6, 132.4, 133.1, 142.5, 143.0, 171.9: MS (positive mode): m/z = 321 $[M + H]^{+2}$. Anal. Calcd (%) for $C_{19}H_{13}N_3O$: C, 76.24; H, 4.38; N, 14.04 Found: C, 76.20; H, 4.35; N, 13.28.

2-(2-(4-Methoxyphenyl)-2′-oxospiro[cyclopropane-1,3′-indolin]-3-yl)malononitrile (8g). White solid, yield = (90%); mp 171–173°C, IR (KBr) (ν_{max}/cm^{-1}): 3221, 3031, 2992, 2326, 1725, 1728, 1642, 1468, 1345, 1278, 1176, 1105, 1057, 877, 673 cm^{-1}; ^{1}H-NMR (400 MHz, $CDCl_3$/TMS): δ 3.87 (s, 1H, CH), 3.57 (s, 3H, CH_3), 6.85–6.88 (m, 2H, Ar–H), 7.18–7.25 (m, 2H, Ar–H), 7.29–7.35 (m, 6H, Ar–H), 9.5 (s, 1H, –NH); ^{13}C-NMR (400 MHz, $CDCl_3$): 18.3, 19.2, 39.3, 42.7, 111.8, 116.2, 115.5, 116.6, 119.3, 120.8, 121.6, 123.8, 124.6, 132.9, 133.5, 143.5, 144.0, 172.9: MS (positive mode): m/z = 316 $[M + H]^{+2}$. Anal. Calcd (%) for $C_{19}H_{13}N_3O_2$: C, 72.37; H, 4.16; N, 13.33 Found: C, 76.27; H, 4.21; N, 13.33.

In silico studies. Docking studies. Molecular docking was used to determine the binding free energy and binding mode of the synthesized compounds **16–22** with DNA gyrase A. Molecular docking was performed with PyRx 0.8 implementation of Auto Dock 4.2 [29] using an empirical free energy force field and Lamarckian genetic algorithm conformational search with the default parameters. The grid box was set around the binding pocket in DNA gyrase A with a 45, 942, and 946 Å grid box having 0.375 Å grid point spacing.

Target structure and ligand dataset preparation. The three-dimensional coordinates of the crystal structure DNA gyrase A were selected from the RCSB Protein Data Bank (PDB code: 3LPX) as the receptor model [30]. Water molecules and hetero atoms were removed from the co-crystal structure. Hydrogen atoms and Gasteiger partial charges were added to the target protein using UCSF Chimera 1.10.2 [31]. The compounds were subjected to energy minimization using the Open Babel module in PyRx program.

In silico *absorption, distribution, metabolism, and excretion prediction.* The synthesized compounds were subjected to prediction of ADME properties. The various ADME properties including TPSA, molecular weight, number of rotatable bonds, molecular volume, number of hydrogen bond donors, number of hydrogen bond acceptors, miLog *P*, and violations of Lipinski rule were calculated by the Mol inspiration online property toolkit. %ABS was calculated by using the formula: %ABS = 109 − (0.3459 TPSA) [32]. ADME prediction properties like %HIA, Caco-2 permeability, %PPB, and BBB were predicted by using pre-ADMET online server (http://preadmet.bmdrc.org/).

Structure–activity relationship studies. The detailed analysis of the structure of spirooxindole compounds is envisaging that the compound exhibits equilibrium due to enolization, where both the isomers are in dynamic interconversion from one form to another. Here, the indolyl nitrogen atom is adjunction point for the continuous conjugation in the indole moiety and phenyl-substituted cyclopropyl spiro system. In this way, nitrogen is protecting the continuous conjugation of π-electron density over entire molecule with its empty p orbital and remaining SP^2 orbitals of carbon atoms. Hence, this is creating two active groups –NH and –OH that are acting as hydrogen bond donors to the active proteins of DNA gyrase A.

The detailed structure–activity relationship study had revealed that active amino-acid ending groups of Asp 104, Glu 139, Tyr 50, Met 101, Val 103, Glu 141, Arg 126, Glu 139, Tyr 50, and Phe 213 are strongly binding with the –NH group of the spirooxindole compounds in structure I, and Asp 104 and Trp 59 are strongly binding with the –OH group of the

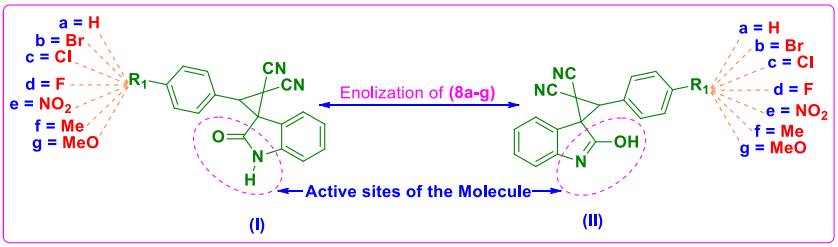

Figure 3. Structure–activity relationship analysis for compounds **8a–g** for binding with DNA gyrase A. [Color figure can be viewed at wileyonlinelibrary.com]

spirooxindole compounds in structure II, respectively, and establishing −7.2 to −6.4 kcal/mole of binding energy. This is making these molecules active and competent to act as potent antibacterial agents as revealed by the molecular docking and other *in silico* parameters. The remaining molecular docking and Lipinski properties are also supporting this type of molecular interaction of the molecules with the target proteins and supporting them to report as antibacterial agents (Fig. 3).

Acknowledgments. We acknowledge the University Grants Commission (UGC), New Delhi, India, for providing the laboratory facilities at Prof. R. Nagarajan's research laboratory, School of Chemistry, University of Hyderabad, Hyderabad, to work under Visiting Researcher Programme of UGC Networking Resource Center Program.

REFERENCES AND NOTES

[1] (a) Xia, M.; Ma, R. Z. J. Heterocyclic Chem 2014, 51, 539; (b) Cheng, D.; Ishihara, Y.; Tan, B.; Barbas, C. F. ACS Catal 2014, 4, 743; (c) Trost, B. M.; Bringley, D. A.; Zhang, T.; Cramer, N. J Am Chem Soc 2013, 135, 16720; (d) Hanhan, N. V.; Ball-Jones, N. R.; Tran, N. T.; Franz, A. K. Angew Chem Int Ed 2012, 51, 989; (e) Dugal-Tessier, J.; O'Bryan, E. A.; Schroeder, T. B. H.; Cohen, D. T.; Scheidt, K. A. Angew Chem Int Ed 2012, 51, 4963; (f) Ball-Jones, N. R.; Badillo, J. J.; Franz, A. K. Org Biomol Chem 2012, 10, 5165; (g) Madin, A.; O'Donnell, C. J.; Oh, T.; Old, D. W.; Overman, L. E.; Sharp, M. J. J Am Chem Soc 2005, 127, 18054.

[2] (a) Hong, L.; Wang, R. Adv Synth Catal 2013, 355, 1023; (b) Ball-Jones, N. R.; Badillo, J. J.; Franz, A. K. Org Biomol Chem 2012, 10, 5165; (c) Cao, Z.-Y.; Wang, Y.-H.; Zeng, X.-P.; Zhou, J. Tetrahedron Lett 2014, 55, 2571; (d) Liu, Y. L.; Wang, X.; Zhao, Y. L.; Zhu, F.; Zeng, X. P.; Chen, L.; Wang, C. H.; Zhao, X. L.; Zhou, J. Angew Chem Int Ed 2013, 52, 13735.

[3] (a) Singh, G. S.; Desta, Z. Y. Chem Rev 2012, 112, 6104; (b) Ball-Jones, N. R.; Badillo, J. J.; Franz, A. K. Org Biomol Chem 2012, 10, 5165; (c) Hong, L.; Wang, R. Adv Synth Catal 2013, 355, 1023.

[4] Yong, S. R.; Williams, M. C.; Pyne, S. G.; Ung, A. T.; Skelton, B. W.; White, A. H.; Turner, P. Tetrahedron 2005, 61, 8120.

[5] Franke, A.; Liebigs, A. Chem 1978, 5, 717.

[6] (a) Jaegli, S.; Vors, J.-P.; Neuville, L.; Zhu, J. Tetrahedron 2010, 66, 911; (b) Wurz, R. P.; Lin, W.; Charette, A. B. Tetrahedron Lett 2003, 44, 8845; (c) Brackmann, F.; de Meijere, A. Chem Rev 2007, 107, 4538; (d) Yankee, E. W.; Spencer, B.; Howe, N. E.; Cram, D. J. J Am Chem Soc 1973, 95, 4230; (e) Gnad, F.; Reiser, O. Chem Rev 2003, 103, 1603.

[7] (a) Kokkinos, A. M. P.; Hassila, H. Acta Chem Scand 1996, 50, 323; (b) Flann, C. J.; Overman, L. E.; Sarkar, A. K. Tetrahedron Lett 1991, 32, 6993; (c) Benson, D. A.; Karsch-Mizrachi, I.; Shanmugam, P. Tetrahedron 2006, 62, 4342.

[8] (a) Deng, H. P.; Wei, Y.; Shi, M. Org Lett 2011, 13, 3348; (b) Zhang, X. C.; Cao, S. H.; Wei, Y.; Shi, M. Chem Commun 2011, 47, 1548.

[9] Presset, M.; Mohanan, K.; Hamann, M.; Coquerel, Y.; Rodriguez, J. Org Lett 2011, 13, 4124.

[10] Girija, S.; Singh, Z.; Desta, Y. Chem Rev 2012, 112, 6104.

[11] (a) Bonavent, G.; Causse, M.; Guitard, M.; Fraisse-Jullien, R. Bull Soc Chim Fr 1964 2462; (b) Epstein, J. W.; Rabander, H. J.; Fanshawe, W. J.; Hofmann, C. M.; McKenzie, T. C.; Safir, S. R.; Osterberg, A. C.; Cosulich, D. B.; Lovell, F. M. J Med Chem 1981, 24, 481; (c) Mangelinckx, S.; De Kimpe, N. Tetrahedron Lett 2003, 44, 1771.

[12] Sun, W.; Zhu, G.; Wu, C.; Hong, L.; Wang, R. Eur J Chem 2012, 18, 6737.

[13] Albertshofer, K.; Tan, B.; Barbas, C. F. Org Lett 2012, 14, 1834.

[14] Tan, B.; Candeias, N. R.; Barbas, C. F. Nat Chem 2011, 3, 473.

[15] Chen, W. B.; Wu, Z. J.; Pei, Q. L.; Cun, L. F.; Zhang, X. M.; Yuan, W. C. Org Lett 2010, 12, 3132.

[16] Jiang, K.; Jia, Z. J.; Yin, X.; Wu, L.; Chen, Y. C. Org Lett 2010, 12, 2766.

[17] Bencivenni, G.; Wu, L. Y.; Mazzanti, A.; Giannichi, B.; Pesciaioli, F.; Song, M. P.; Bartoli, G.; Melchiorre, P. Angew Chem 2009, 121, 7336.

[18] Duan, S. W.; Li, Y.; Liu, Y. Y.; Zou, Y. Q.; Shi, D. Q.; Xiao, W. J. Chem Commun 2012, 48, 5160.

[19] Artur Noole, N.; Sucman, S.; Mikhail, A.; Kabeshov, T.; Kanger Fliur, Z.; Macaev, A.; Malkov, V. Eur J Chem 2012, 18, 14929.

[20] Artur, N.; Andrei, V.; Malkov, T. K. Synthesis 2013, 45, 2520.

[21] Erin, E.; Wilson, K.; Rodriguez, X.; Brandon, L. A. Tetrahedron 2015, 71, 5765.

[22] Rong, Z.; Changjiang, Y.; Yiyi, L.; Ruifeng, L.; Zhengjie, H. J Org Chem 2014, 79, 10709.

[23] Wen-Jie, Q.; Ying, H.; Chao-Guo, Y. Tetrahedron 2016, 72, 5057.

[24] John, L.; Alexandra, W.; Holubec, A.; Brian, M.; Matthew, S.; Weiss, M.; Julie, A.; Brian, D.; Doan, D.; Mohammed, F.; Jennifer, S.; Chen, M.; Timothy, P. H. J Am Chem Soc 1999, 121, 6326.

[25] Yuan, L.; Yu-Liang, W.; Yi-Ying, Z. Asian J Chem 2015, 27, 491.

[26] Xiaoqiu, P.; Qingwei, L.; Zehai, L.; Xianjin, Y. Eur J Org Chem 2016, 5937.

[27] Morris, G. M.; Huey, R.; Lindstrom, W.; Sanner, M. F.; Belew, R. K.; Goodsell, D. S.; Olson, A. J. J Comput Chem 2009, 30, 2785.

[28] Haar, E.; Coll, J. T.; Austen, D. A.; Hsiao, H. M.; Swenson, L.; Jain, J. Nat Struct Biol 2009, 8, 593.

[29] Pettersen, E. F.; Goddard, T. D.; Huang, C. C. J Comput Chem 2004, 25, 1605.
[30] Zhao, Y.; Abraham, M. H.; Lee, J.; Hersey, A.; Luscombe, N. C.; Beek, G.; Sherborne, B.; Cooper, I. Pharm Res 2002, 19, 1446.
[31] Lipinski, C. A.; Lombardo, F.; Dominy, B. W.; Feeny, P. J. Adv Drug Deliv Rev 1997, 23, 3.
[32] Clark, D. E.; Pickett, S. D. Drug Discov 2000, 5, 49.

SUPPORTING INFORMATION

Additional supporting information may be found online in the Supporting Information section at the end of the article.